SUPPLEMENTARY INFORMATION

Epitranscriptomic regulation of cortical neurogenesis via Mettl8-dependent mitochondrial tRNA m^3C modification

Feng Zhang, Kijun Yoon, Daniel Y. Zhang, Nam-Shik Kim, Guo-li Ming and Hongjun Song

Inventory

Figures S1-4

Tables S1-3

SUPPLEMENTARY FIGURES

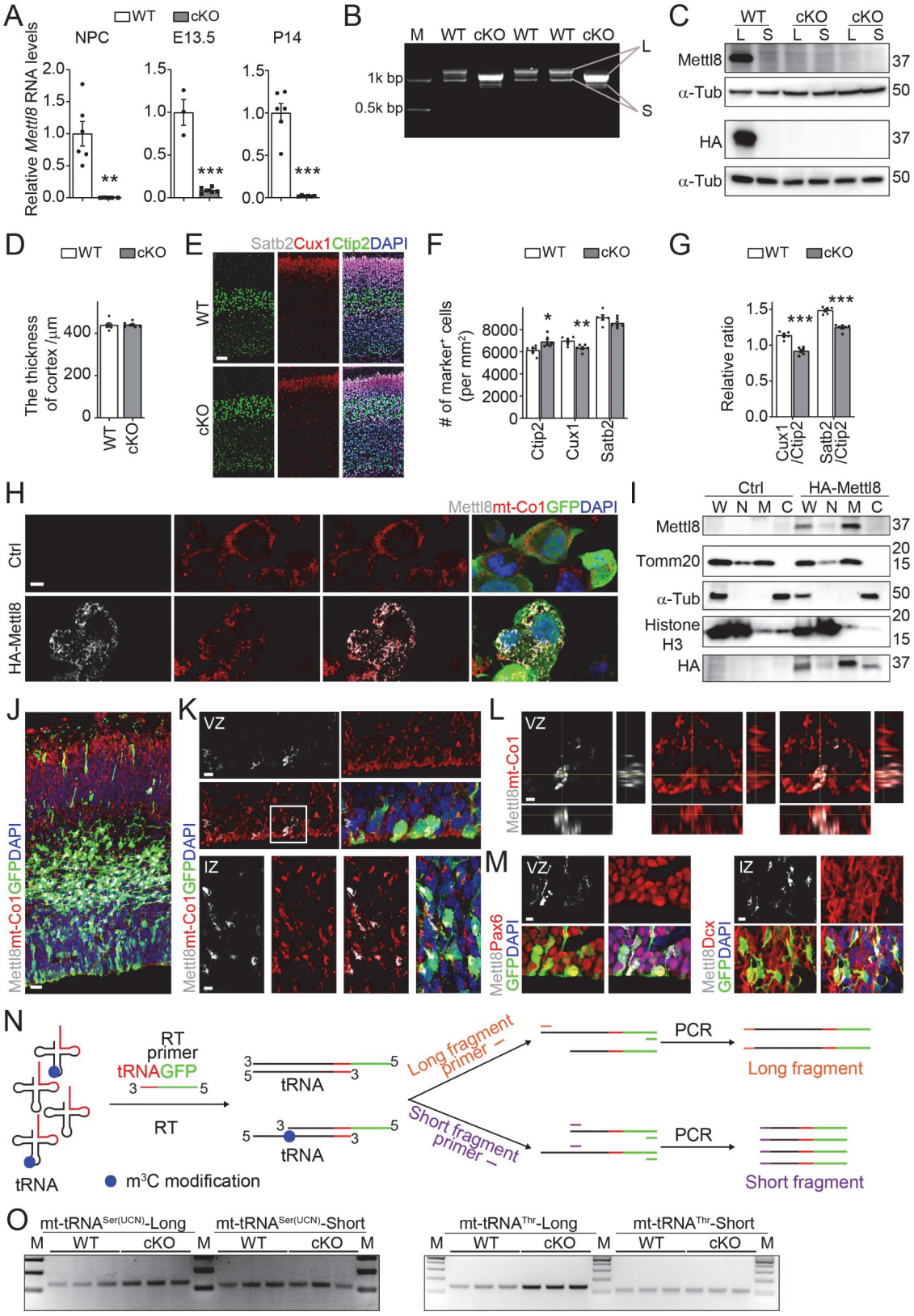

Figure S1. Characterization of *Mettl8* cKO mice, Mettl8 localization and a qPCR-based method for analysis of m^{3}C modification of tRNAs, related to Figure 1

(**A**) Deletion of exon 3 of the *Mettl8* gene in the cKO mouse brain. The mRNA levels of Exon 3 of *Mettl8* gene in NPCs generated from E17.5 WT and cKO embryonic cortex and in the E13.5 and P14 WT and cKO cortex were determined with qPCR. *β-Actin* was used as an internal control for normalization. Values represent mean ± SEM (NPCs: n = 6/WT; n = 5/cKO; E13.5 cortex: n = 4/WT; n = 5/cKO; P14 cortex: n = 6/WT; n = 6/cKO; **P < 0.01, ***P < 0.001; Student's *t*-test).
(B-C) Only the long isoform of *Mettl8* gene from the WT mouse brain can make Mettl8 protein. Shown in (**B**) is a sample gel image of PCR-amplified *Mettl8* gene, exhibiting long (L) and short (S) isoforms in both WT and cKO samples. Shown in (**C**) are the sample Western blot images for Mettl8, HA and α-Tub (as the loading control) from HEK293 cells transfected with pCAGIG plasmids expressing long/short isoform of C-terminal HA-tagged Mettl8 cloned from WT and cKO cDNA.
(D-G) Altered cortical neurogenesis in the cKO mice. Shown are the summary of cortical thickness (**D**) and sample confocal images of immunostaining for Ctip2 (a deep-layer neuron marker), Cux1 and Satb2 (superficial-layer neuron markers), and DAPI in WT and cKO mice at P1 (**E**; Scale bar: 50 μm) and quantification of the density of $Ctip2^+$ cells, $Cux1^+$ cells and $Satb2^+$ cells **(F)** and ratios of $Cux1^+/Ctip2^+$ cells and $Satb2^+/Ctip2^+$ cells **(G)** in WT and cKO mice at P1. Values represent mean ± SEM (n = 6/WT; n = 6/cKO; **P < 0.01, ***P < 0.001; Student's *t*-test).
(H-I) Localization of Mettl8 in mitochondria of mouse N2a cells. Shown in (**H**) are sample confocal images of immunostaining for Mettl8, mitochondria marker mt-Co1 and GFP in N2a cells transfected with pCAGIG plasmid expressing GFP or pCAGIG-HA-Mettl8 plasmids co-expressing Mettl8 and GFP. Scale bar, 5 μm. Shown in (**I**) are sample Western blot images of different biochemical fractions, including whole cell lysates (W), nucleus (N), mitochondria (M) and cytosol (C) of N2a cells transfected with pCAGIG or pCAGIG-HA-Mettl8 plasmids, blotting Mettl8, Histone H3 (nucleus marker), Tomm20 (mitochondria marker), α-tubulin (cytosol marker) and HA.
(J-M) Localization of overexpressed Mettl8 in the mitochondria of neural stem cells and neurons in the embryonic mouse brain upon *in utero* electroporation with pCAGIG-Mettl8 plasmids at E13.5 and analysis at E15.5. Shown are sample confocal images of immunostaining for Mettl8, mt-Co1 and GFP in mouse cortex at E15.5 (**J**; Scale bar: 20 μm) with enlarged views of the ventricular zone (VZ, upper panel) and intermediate zone (IZ, lower panel) (**K**; Scale bar: 5 μm) and enlarged 3D views of the ventricular zone (**L**; Scale bar: 2 μm). Also shown are sample confocal images of immunostaining for Mettl8, Pax6 (a neural stem cell marker) and GFP in the ventricular zone (VZ, upper panels) and Mettl8, Dcx (an immature neuronal marker) and GFP in the intermediate zone (IZ, lower panels) (**M**; Scale bar: 5 μm).
(N) Schematic diagram showing the design of m^3C modification detection by qPCR. The m^3C modification can block the reverse transcription (RT), resulting in the generation of both long (without modification) and short (with modification) fragments of cDNA from tRNA during RT when using tRNA RT primer, which has the reverse complement sequence of 3' fragment of tRNA plus one 72bp fragment of GFP. For qPCR, short primer sets could detect both long and short fragments, while long primer sets can only detect long fragments. The value of $2^{(\text{the difference of CT values got by qPCR when using short and long primer sets})}$, short for long/short value, could indicate the m^3C modification level. The higher the long/short value, the lower the m^3C modification level.
(O) Sample agarose gel images of PCR-amplified long and short fragments of cDNA from mt-$tRNA^{Ser(UCN)}$ and mt-$tRNA^{Thr}$ in WT and cKO mouse brains at P14 using specific qPCR primer sets for long and short fragments as illustrated in (**N**). M: DNA markers.

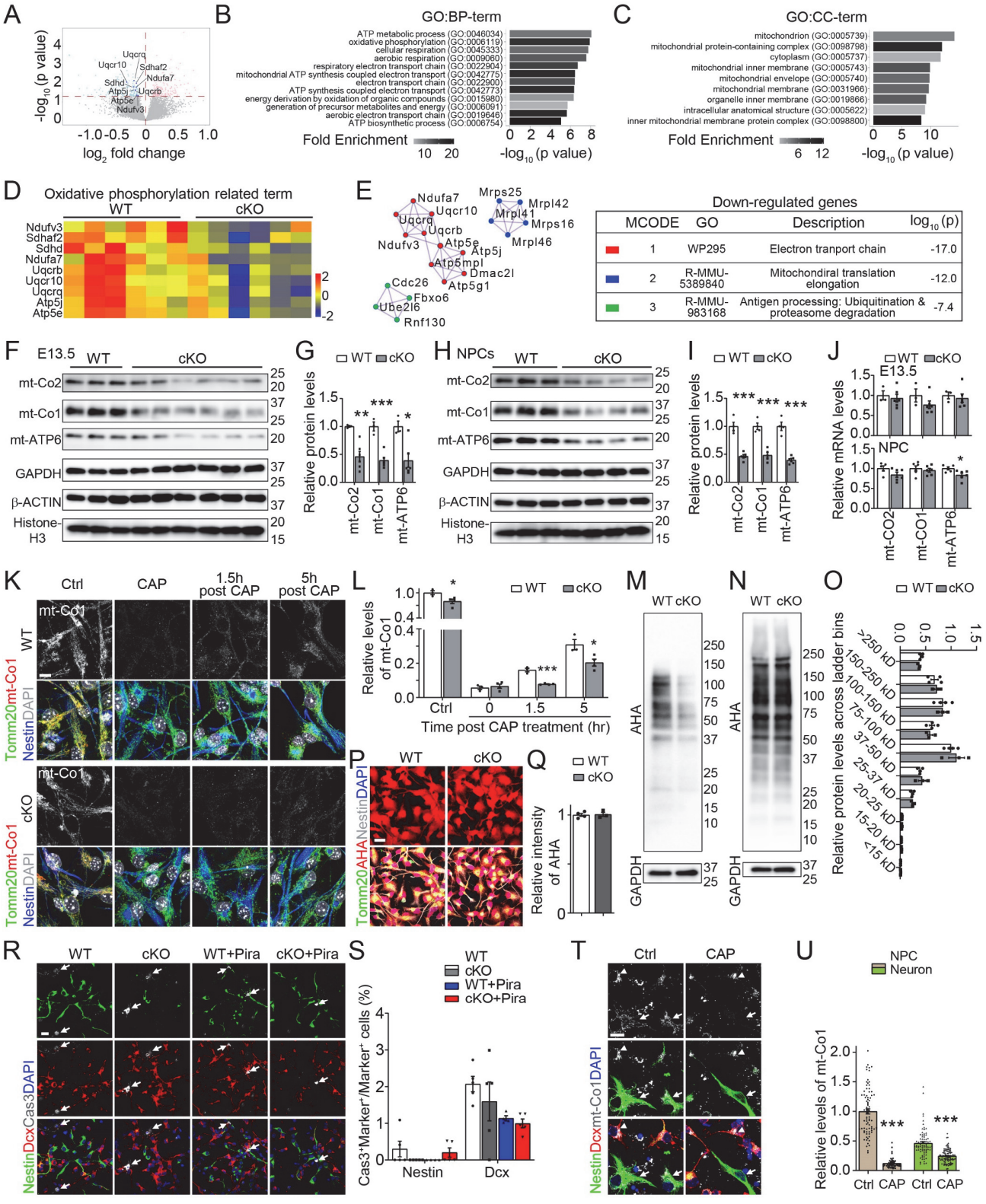

Figure S2. *Mettl8* deletion in NPCs impacts gene expression related to mitochondria and impairs mitochondria protein translation, related to Figures 1 and 2

(A-E) Differential gene expression between NPCs from E17.5 WT and *Mettl8* cKO embryonic mouse cortex. Shown in (**A**) is a Volcano plot of differentially expressed genes from the RNA-seq analysis. Significantly downregulated and upregulated genes (P value < 0.05) are indicated by blue and red dots. Downregulated genes in the oxidative phosphorylation related term are indicated. Also shown are bar plots of enriched gene ontology (GO) terms for biological process (**B**) and for cellular component (**C**) of downregulated genes in *Mettl8* cKO compared to WT NPCs. Shown in (**D**) is a heatmap of downregulated genes related to the oxidative phosphorylation term in *Mettl8* cKO compared to WT NPCs. Values are shown as the row Z-score of normalized gene counts of listed genes for each biological replicate. Shown in (**E**) are diagrams of constructed protein-protein interaction networks of downregulated genes in cKO compared to WT NPCs and enriched pathways of identified MCODE components analyzed by Metascape.
(F-I) Decreased mitochondria proteins in E13.5 cerebral cortex (**F-G**) and cultured NPCs (**H-I**) in cKO compared to WT samples. Shown are sample Western blot images (**F, H**) for mt-Co2, mt-Co1, mt-ATP6, GAPDH (as the loading control), β-Actin and Histone-H3, and quantifications (**G, I**). The intensity of mt-Co2, mt-Co1, and mt-ATP6 bands was normalized with that of GAPDH and then compared to WT samples. Values represent mean ± SEM (E13.5 cortex: n = 3/WT; n = 6/cKO; NPCs: n = 4/WT; n = 5/cKO; *P < 0.05, **P < 0.01, ***P < 0.001; Student's *t*-test).
(J) Transcription of mitochondria genome encoding genes were largely unaffected by *Mettl8* deletion. The mRNA levels of *mt-Co1, mt-Co2* and *mt-ATP6* in the E13.5 cerebral cortex and NPCs from WT and cKO mice were quantified by qPCR. *β-Actin* was used as an internal control for normalization. Values represent mean ± SEM (E13.5 cortex: n = 3/WT; n = 6/cKO; NPCs: for mt-Co1: n = 6/WT; n = 6/cKO; for mt-Co2 and mt-ATP6: n = 5/WT; n = 6/cKO; *P < 0.05; Student's *t*-test).
(K-L) Reduced *de novo* mitochondria protein synthesis in cKO compared to WT NPCs. NPCs from WT and cKO mice were treated with saline (ctrl) or CAP (10 μg/mL) for 48 hours and then examined at 1.5 hours and 5 hours after the removal of CAP. Shown are sample confocal images of immunostaining for mt-Co1, Tomm20 and Nestin at different time points (**K**; Scale bar: 10 μm) and quantification of the relative intensity of mt-Co1 levels (**L**). Values represent mean ± SEM (n = 3/WT; n = 4/cKO; *P < 0.05; ***P < 0.001; Student's *t*-test).
(M) Mitochondrial protein translation in NPCs was reduced by *Mettl8* deletion. WT and cKO NPCs were first cultured in the media without Methionine for 1.5 hours, and then treated with cycloheximide (50 μg/mL) for 0.5 hour, followed by culture in Methionine-depleted media containing cycloheximide and AHA (500 μM) for 3 hours. Shown are sample Western blot images for AHA and GAPDH (as loading controls).
(N-Q) Cytosolic protein translation in NPCs was not affected by *Mettl8* deletion. WT and cKO NPCs were first cultured in the media without Methionine for 1.5 hours, and then treated with CAP (10 μg/mL) for 0.5 hour, followed by culture in Methionine-depleted media containing CAP and AHA (500 μM for **M-N** and 300 μM for **O-P**) for 3 hours. Shown are sample Western blot images (**N**) for AHA and GAPDH (as loading controls) and quantification of the intensity of AHA bands between marker bins normalized with that of GAPDH (**O**). Values represent mean ± SEM (n = 4/WT; n = 3/cKO). Also shown are sample confocal images of immunostaining for AHA, Tomm20, Nestin and DAPI (**P;** Scale bar, 10 μm) and quantification of the relative intensity of AHA signal in WT and cKO NPCs (**Q**). Values represent mean ± SEM (n = 4/WT; n = 3/cKO).
(R-S) Minimal cell death in different culture conditions. Shown are sample confocal images for cleaved-Caspase3, Nestin and Dcx in WT and cKO NPCs with or without piracetam (Pira, 1 mM) treatment for 48 hours (**R**; Scale bar: 20 μm) and quantification of percentages of $Caspase3^+Nestin^+$ NPCs among all $Nestin^+$ NPCs and percentages of $Caspase3^+Dcx^+$ cells among all Dcx^+ cells in different conditions (**S**). Arrows point to $Caspase3^+$ cells. Values represent mean ± SEM (n = 5/WT; n = 5/cKO; n = 4/WT+Pira; n = 5/cKO+Pira).
(T-U) Effectiveness of mitochondria protein translation inhibitor CAP in NPC cultures. Shown are sample confocal images of immunostaining for mt-Co1, Dcx and Nestin in primary NPC cultures from CD1 mice and treated with vehicle (ctrl) or CAP (10 μg/mL) for 48 hours (**T**; Scale bar: 10 μm)

and quantification of the relative signal intensity of mt-Co1 (**U**). Arrowheads and arrows point to DCX^+ and $Nestin^+$ cells, respectively. Values represent mean ± SEM (NPC-Ctrl: n = 80 cells from 4 mice; NPC-CAP: n = 51 cells from 4 mice; Neuron-Ctrl: n = 78 cells from 4 mice; Neuron-CAP: n = 105 cells from 4 mice; ***P < 0.001; One-way ANOVA).

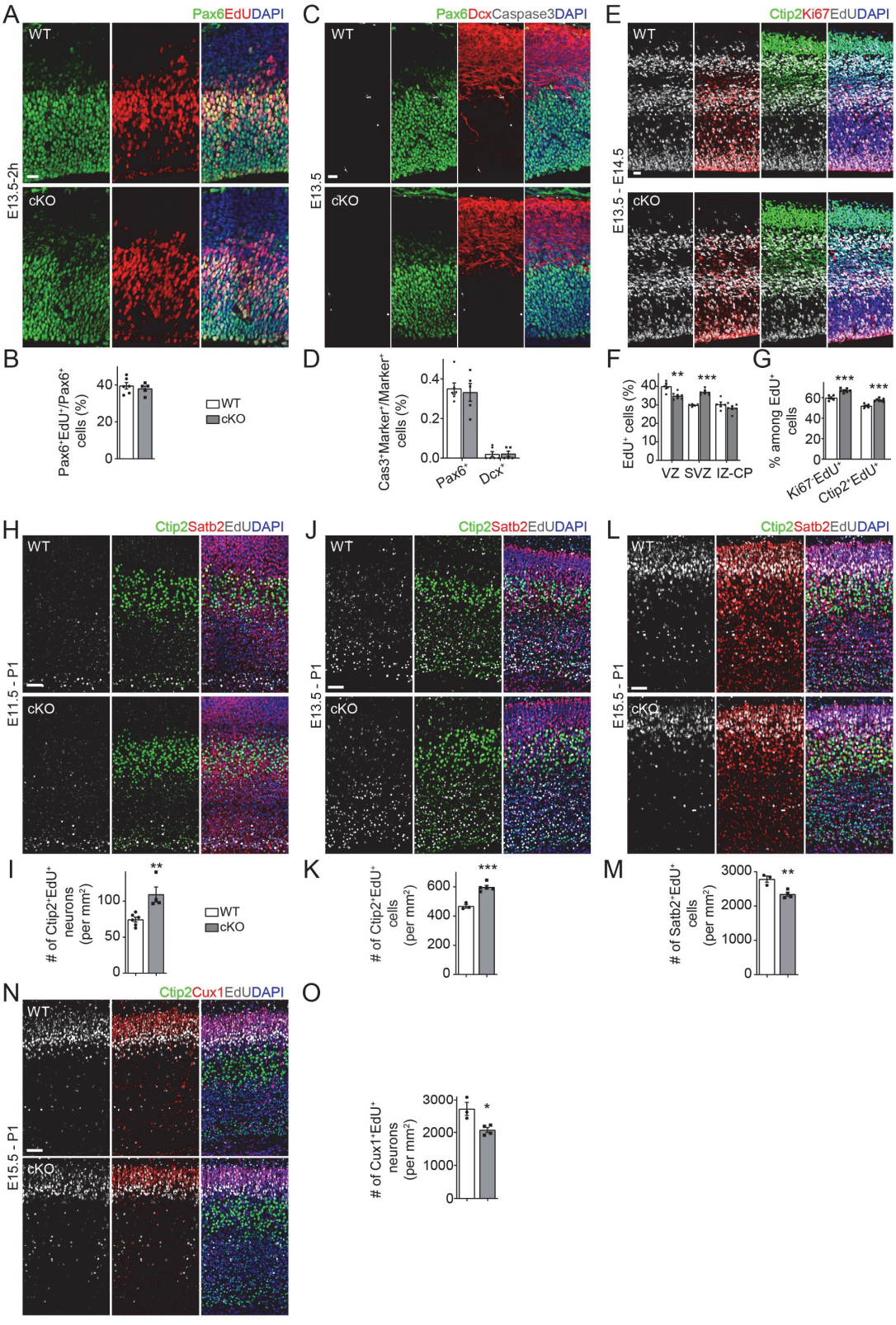

Figure S3. *Mettl8* cKO mice exhibit deficits in neural stem cell maintenance and changes in generation of neurons of deep- and superficial-layers during embryonic cortical development, related to Figure 3

(A-B) *Mettl8* deletion did not affect neural stem cell proliferation *in vivo*. WT and cKO mice were injected with EdU (16.7 mg/Kg body weight) at E13.5 and analyzed 2 hours later. Shown are sample confocal images of immunostaining for Pax6, EdU and DAPI (**A**; Scale bar: 20 μm) and quantification of percentages of EdU^+Pax6^+ cells among all $Pax6^+$ cells in WT and cKO cortex (**B**). Values represent mean ± SEM (n = 6/WT; n = 5/cKO).
(C-D) *Mettl8* deletion did not affect cell survival *in vivo*. Shown are sample confocal images of immunostaining for cleaved-Caspase3, Dcx, Pax6 and DAPI (**C**; Scale bar: 20 μm) and quantification of the percentage of $Caspase3^+Pax6^+$ among $Pax6^+$ cells and the percentage of $Caspase3^+Dcx^+$ among Dcx^+ cells in WT and cKO cortex at E13.5 (**D**). Values represent mean ± SEM (n = 6/WT; n = 5/cKO).
(E-G) *Mettl8* cKO mice exhibit enhanced cell cycle exit and neuronal differentiation in the embryonic mouse cortex. WT and cKO mice were injected with EdU (16.7 mg/Kg body weight) at E13.5 and analyzed at E14.5. Shown are sample confocal images of immunostaining for Ki67 (proliferation marker), Ctip2 (deep layer neuron marker), EdU and DAPI (**E**; Scale bar: 10 μm) and quantification of percentages of EdU^+ cells distributed across different layers of the cortex (**F**) and percentages of EdU^+Ki67^- cells and EdU^+Ctip2^+ neurons (**G**) among all EdU^+ cells in WT and cKO cortex. Values represent mean ± SEM (n = 5/WT; n = 7/cKO; $^{**}P < 0.01$, $^{***}P < 0.001$; Student's *t*-test).
(**H-O**) *Mettl8* cKO mice exhibit altered generation of deep-layer and superficial-layer neurons during embryonic cortical development. WT and cKO mice were injected with EdU (16.7 mg/Kg body weight) at E11.5, E13.5, or E15.5, and analyzed at P1. Shown are sample confocal images (Scale bars: 50 μm) of immunostaining for Ctip2, Satb2, Cux1, EdU and DAPI in WT and cKO mice injected with EdU at E11.5 (**H**), E13.5 (**J**) and E15.5 (**L, N**) and quantification of the density of $Ctip2^+EdU^+$ cells, $Ctip2^+EdU^+$ cells, $Satb2^+EdU^+$ cells and $Cux1^+EdU^+$ cells at P1 of WT and cKO mice injected with EdU at E11.5 (**I**), E13.5 (**K**), E15.5 (**M**) and E15.5 (**O**), respectively. Values represent mean ± SEM (E11.5: n = 6/WT; n = 4/cKO; E13.5: n = 3/WT; n = 5/cKO; E15.5: n = 3/WT; n = 4/cKO; $^{*}P < 0.05$, $^{**}P < 0.01$, $^{***}P < 0.001$; Student's *t*-test).

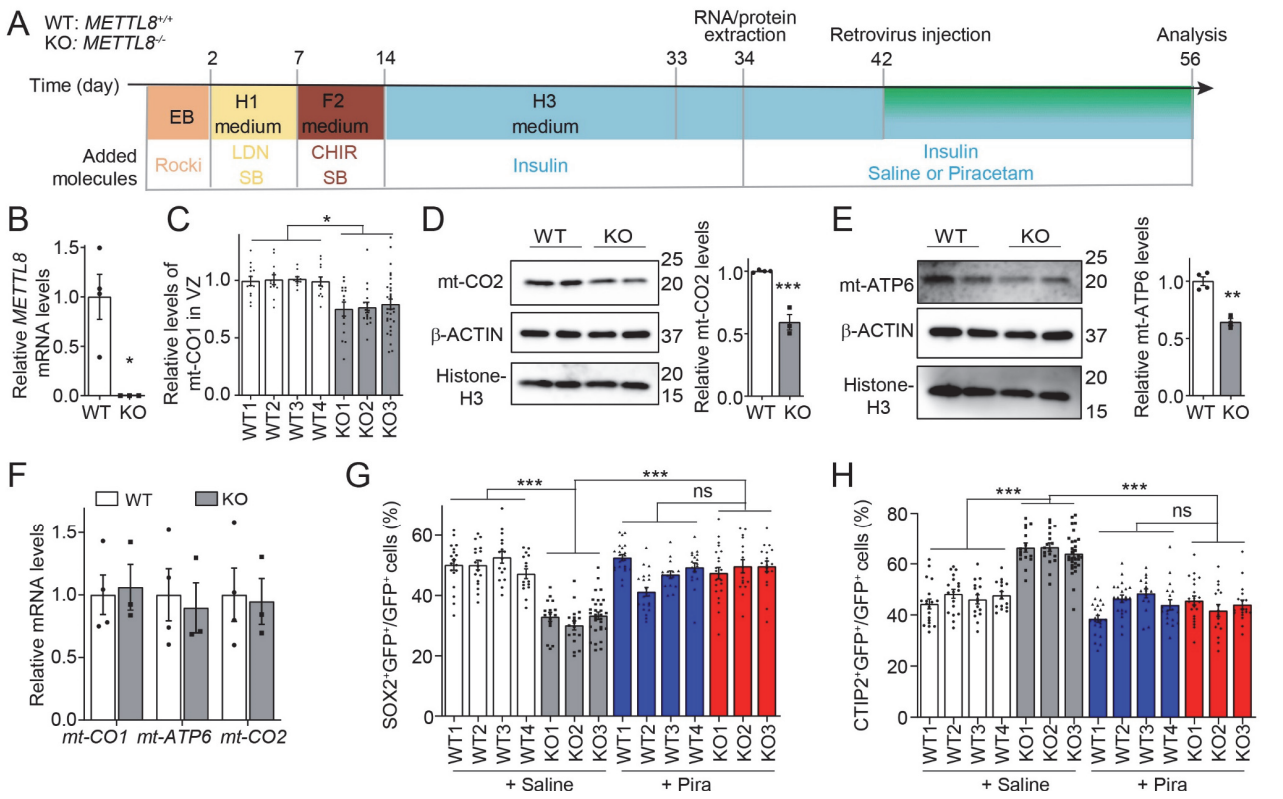

Figure S4. *METTL8* KO human forebrain organoids exhibit decreased mitochondria protein expression, and deficits in radial glia neural stem cell maintenance with increased neuronal differentiation, related to Figure 4

(A) A schematic diagram of human forebrain organoid generation, experimental procedures and drug treatment scheme.

(B) Deletion of Exon 3 of the *METTL8* gene in KO organoids. The mRNA levels of Exon 3 of *METTL8* gene in WT and KO organoids at D33 were quantified by qPCR with *GAPDH* used as the internal control. Individual dots represent data from organoids derived from each iPSC line. Values represent mean ± SEM (n = 4 WT iPSC lines; n = 3 KO iPSC lines; *P < 0.05; Student's *t*-test).

(C) Reduced mt-CO1 levels in the VZ of KO forebrain organoids. The same data as in **Figure 4D** plotted for individual iPSC lines. Each dot represents data from each rosette. Values represent mean ± SEM (n = 13/WT1; n = 12/WT2; n = 10/WT3; n = 13/WT4; n = 14/KO1; n = 16/KO2; n = 31/KO3; *P < 0.05; One-way ANOVA).

(D-E) Reduced levels of mt-CO2 and mt-ATP6 in KO compared to WT organoids at D33. Shown are sample Western blot images for blotting mt-CO2, mt-ATP6, Histone-H3 and β-ACTIN (as loading controls) and quantifications. The relative intensity of mt-CO2 (**D**) and mt-ATP6 (**E**) bands normalized with that of β-ACTIN was used for quantification. Values represent mean ± SEM (n = 4/WT; n = 3/KO; **P < 0.01, ***P < 0.001; Student's *t*-test).

(F) *METTL8* deletion did not impact the transcription of mitochondria genome-encoding genes. The mRNA levels of *mt-CO1*, *mt-ATP6* and *mt-CO2* in WT and *METTL8* KO organoids at D33 were quantified by qPCR. Values represent mean ± SEM (n = 4/WT; n = 3/KO).

(**G-H**) Decreased percentages of neural stem cells and increased percentages of neurons in *METTL8* KO compared to WT organoids at D56 and rescue by piracetam treatment (1 mM). Same data as in **Figures 4F-G** plotted for individual iPSC lines. Each dot represent data from each section. Values represent mean ± SEM (n = 19/WT1; n = 18/WT2; n = 16/WT3; n = 15/WT4; n = 16/KO1; n = 18/KO2; n = 30/KO3; n = 22/WT1+Pira; n = 21/WT2+Pira; n = 15/WT3+Pira; n =

18/WT4+Pira; n = 22/KO1+Pira; n = 16/KO2+Pira; n = 18/KO3+Pira; ns: P>0.05, ***P < 0.001; One-way ANOVA).

SUPPLEMENTARY TABLES (IN EXCEL FILES)

Table S1. List of PCR primers and DNA oligos used in the current study, related to Figures 1 and 4.

Table S2. Summary of m^3C-HAC-seq analysis of WT and *Mettl8* cKO NPCs, related to Figure 1. Shown is the list of the cleavage ratio of analyzed Cytosine sites with more than one read in each WT sample in m^3C-HAC-seq starting at their +1 bp downstream sites.

Table S3. Lists of differentially expressed genes, and their GO terms and PPI modules in NPCs between WT and *Mettl8* cKO NPCs, related to Figures 1 and 2.